Lung Vascular Permeability: Inferences from Measurements of Plasma to Lung Lymph Protein Transport[1]

K.L. Brigham, M.D.[2], Th.R. Harris, M.D., Ph.D., R.E. Bowers, M.D., R.J. Roselli, Ph.D.

Pulmonary Circulation Center, Vanderbilt University School of Medicine, Nashville, Tennessee 37232

Summary

In chronically instrumented unanesthetized sheep, we measured steady-state hemodynamic and lung lymph responses to mechanically increased pressure and to intravenous infusions of histamine, Pseudomonas bacteria and E. coli endotoxin. Histamine, Pseudomonas bacteria and E. coli endotoxin caused exchanging vessel permeability to increase, as evidenced by high flows of protein rich lung lymph. This contrasts to the effects of increased pressure where lymph protein concentration falls as lymph flow increases. Microvascular sieving of proteins less than 100 A radius persisted in all increased permeability states, but with endotoxin, lymph clearance of larger proteins increased much more than with histamine or Pseudomonas. We compared several approaches to quantitative interpretations of lymph data and found that direct methods for calculating permeability-surface area products and reflection coefficients for proteins produced values which were difficult to interpret, probably because fundamental assumptions of the methods were violated in our experiments. A mathematical model based on multiple pore theory produced more plausible coefficients.

If lymph flow from an organ is net transvascular fluid movement and lymph protein concentrations are the same as those of the microvascular filtrate (reasonable assumptions in the steady-state; 1, 2, 3), then inferences about the function and structure of exchanging vessel walls can be made from lymph measurements (1, 4, 5, 6, 7, 8, 9).

We measured lung lymph flow and lymph and plasma concentrations of eight endogenous protein fractions with Einstein-Stokes radii 35.5–96 Å in sheep in a variety of steady-state conditions. We found that permeability could increase while exchanging vessels still sieved proteins and that the pattern of lymph protein flux as a function of molecular size differed among several insults which increased permeability. We also found that lung exchanging vessels did not behave like a simple homoporous membrane so that, as suggested by others (10, 11), direct inferences of transport coefficients from lymph data were questionable. However, a mathematical model based on multiple pore theory, where pore geometry is assumed and data are fitted, promises specific information about membrane structure.

Experimental Methods

Preparation

We made all of these experiments in yearling sheep prepared as described in earlier publications (5, 6, 12). Through three thoracotomies, we put catheters in the left atrium, pulmonary artery and the efferent duct of the caudal mediastinal lymph node. We put a Foley balloon catheter in the left atrium for elevating left atrial pressures and catheters through neck vessels into the superior vena cava and thoracic aorta. We ligated the tail of the caudal mediastinal lymph node below the lung to eliminate systemic lymph (12).

0024–7766/79 1500–0177 $ 02.00 © Georg Thieme Publishers

Animals recovered and had a stable flow of blood-free lymph by 3–5 days after surgery. Then we did experiments, continuously measuring vascular pressures, recording the volume of lymph collected each fifteen minutes and collecting lymph samples each 30 minutes and blood samples each hour for protein measurements.

Interventions

We studied steady-state responses to mechanically increased pressure (left atrial balloon inflation) and intravenous infusions of histamine, Pseudomonas bacteria and E. coli endotoxin. Earlier we reported results of increased pressure (13), histamine (5), and Pseudomonas studies (14), but some of the data are repeated here for comparison. The experimental protocols are given in the earlier papers (5, 13, 14).

E. Coli Endotoxin: After a stable baseline period, we infused intravenously 0.20 to 1.33 μg/kg E. coli endotoxin (Difco, E. coli 0127:B-8, lot # 3123-25) dissolved in 40 ml 0.9% NaCl solution over 30 minutes. We followed the animals for 6 to 8 hours after infusing endotoxin.

Protein Measurements

We measured total protein concentration in plasma and lymph samples by a modified biuret method (15) using an automated device (Auto Analyzer, Technicon Instruments, Tarrytown, New York); duplicate samples differed by less than five percent.

We have described earlier how we separated eight protein fractions in plasma and lymph samples (5, 6). Briefly, we used 4–30% polyacrylamide gradient gels to separate proteins. By calibrating the gels with five known proteins and plotting migration distance against Einstein-Stokes radius, we generated a standard curve from which the radii of our eight plasma and lymph fractions could be estimated without actually identifying the proteins. Assuming the sum of all fractions equalled the measured total protein concentration, we calculated the concentration of each fraction in each sample (5, 6).

Theoretical Methods

Basic Equations

Exchange of water and hydrophilic solutes may occur through a variety of pathways: cellular membrane pores; intracellular pores, clefts or gaps; micropinocytotic vesicles (16). The relative importance of these pathways in lung microvessels is not clear. However, a body of theory for the description of vascular to lymph transport does exist.

The membrane transport theory of *Kedem* and *Katchalsky* (17) is the basis of equations which have been used to analyze blood-to-lymph fluid and protein transport. These equations describe rates of fluid (J_{vi}) and solute flow (J_{si}) through a single pore, i, for water and a single solute, s, as:

$$J_{vi} = L_i (\Delta P - \sigma_{si}\Delta\pi_s) \tag{1}$$

$$J_{si} = PS_{si}\Delta C_s + (1 - \sigma_{si})\bar{C}_s J_{vi} \tag{2}$$

where ΔP and $\Delta\pi_s$ are the differences in hydrostatic pressure and osmotic pressure generated by the solvent concentration gradient across the membrane, ΔC_s is the transmembrane concentration gradient and $\bar{C}_s$ is the arithmetic mean solute concentration within the pore. The three transport coefficients L_i (filtration coefficient), σ_{si} (reflection coefficient) and PS_{si} (permeability coefficient) are required to completely characterize the transport properties of the pore. *Solomon* (18) and *Bean* (19) have reviewed the application of these equations to a variety of biological and physical systems.

For a specific pore geometry, hydrodynamic theories of restricted Stokes flow of solid particles can relate L_i, σ_{si} and PS_{si} to the ratio of molecular size to pore radius (a_s/R_p) (20, 21, 22, 23). If valid for biological membranes, this approach greatly simplifies the analysis of physiological transport data because L_i, σ_{si} and PS_{si} may be interrelated through pore geometry and solute molecular radius.

Although $\bar{C}_s$ in equation (2) has been considered to be the arithmetic average of the s concentrations on either side of the membrane, continuum analysis of the diffusion

problem incorporating bulk flow (21, 23, 24) led to the following restatement of equation (2):

$$J_{si} = J_{vi} \left[(1 - \sigma_{si})C_{sp} + \frac{C_{sp} - C_{sL}}{e^{\beta_{si}} - 1} \right] \quad (3)$$

where

$$\beta_{si} = \frac{J_{vi}(1 - \sigma_{si})}{PS_{si}}$$

C_{sp}, C_{sL} = Plasma and lymph protein concentrations.

In addition, this may be rearranged so that equation (2) is still valid but $\overline{C}_s$ is defined as

$$\overline{C}_s = C_{sL}\,\Theta_{si} + C_{sp}(1 - \Theta_{si}) \quad (4)$$

and

$$\Theta_{si} = \frac{1 + \beta_{si} - e^{\beta_{si}}}{\beta_{si}(1 - e^{\beta_{si}})} \quad (5)$$

Heteroporous Systems

Taylor et al. (10) and *Brace* et al. (11) have recently reexamined the application of equations (1) and (2) to whole-organ transport. In this application L, PS and σ (functional coefficients) describe overall transport of total protein rather than single pore transport of one solute. Thus, equations (1) and (2) are re-written as

$$Q_v = L_0(\Delta P - \sigma_{Pd}\,\Delta\pi_P) \quad (6)$$

$$Q_P = PS_p\Delta C + (1 - \sigma_{Pf})\overline{C}_P Q_v \quad (7)$$

where Q_v is the total transmembrane fluid flow and Q_P is the total transmembrane protein flow. For a homoporous system,

$$\sigma_{Pd} = \sigma_{Pf}$$

and

L_0 = number of pores x L_i

PS_p = number of pores x PS_{Pi}

These authors showed, however, that for a heteroporous system (but a single combined solute, P)

$$PS_p = \Sigma_i N_i PS_{Pi} \quad (8)$$

$$L_0 = \Sigma_i N_i L_{0i} \quad (9)$$

$$\sigma_{Pd} = \frac{\Sigma_i N_i L_{0i}\sigma_{Pi}}{L_0} \quad (10)$$

$$\sigma_{Pf} = \frac{\Sigma_i N_i \sigma_{Pi} J_{vi}}{Q_v} \quad (11)$$

for $\overline{C}_P = (C_{Pp} + C_{PL})/2$ and N_i = total number pores of a given size i.

Organ analysis with these equations leads to four coefficients: L_0, PS_p, σ_{Pf}, σ_{Pd}. As indicated by equation (11), the coefficient σ_{Pf} alters with changes in transmembrane flow.

Taylor et al. (10) used equation (6) and (7) to analyze lymph and protein flow data from several organ systems and found that in general $\sigma_{Pd} \neq \sigma_{Pf}$ and σ_{Pf} altered with lymph flow. They interpreted this to mean that the exchanging vessels of most organs are heteroporous. If multiple solutes (instead of total protein) are considered, the equations become even more complex. No single set of functional coefficients will describe transvascular exchange in an organ for different filtration rates.

Analysis of Experimental Multiple Solute Data

The simplest application of the transport equations to lymph flow of multiple proteins has been based on the approximation of PS obtained by assuming $\sigma_{Pf} = \sigma_{Pd} = 1$ in equations (6) and (7). Then for steady-state in which $Q_s = Q_v C_{sL}$,

$$PS_s^\bullet \equiv \frac{Q_v C_{sL}}{C_{sp} - C_{sL}} \quad (12)$$

and

$$L^\bullet \equiv \frac{Q_v}{\Delta P - \Delta\pi_P} \quad (13)$$

where $PS_s^\bullet$ and $L^\bullet$ are the approximate permeability surface area and filtration coefficients resulting from the assumptions.

If the effective reflection coefficients are not 1, these equations overestimate true protein PS because some convective flow is considered to be diffusive.

Renkin et al. (8, 9) derived an improved version of this equation by rearranging equation (7) into the form:

$$\frac{Q_v C_{sL}}{C_{sp} - C_{sL}} = \frac{PS_s}{\sigma_{sf}} + 1/2(\frac{1}{\sigma_{sf}} - 1)Q_v = PS_s^\bullet \quad (14)$$

They plotted $PS_s^\bullet$ as a function of Q_v for various levels of venous elevation in the isolated dog hind limb. The slope and intercept of the resulting linear plot were used to calculate σ_{sf} and PS_s. Then, by considering multiple pathways of cellular and small intercellular pores ($\sigma = 1$), and large pores ($0 < \sigma < 1$), they inferred the size of the large pores to be 280 Å. This pore size did not explain the PS_s values. The authors interpreted the difference as significant vesicular transport.

Equation (14) neglects the nonlinear nature of $\overline{C}_s$ and further considers σ_{sf} to be constant for various conditions of flow (Q_v) caused by increasing venous pressure. But if the partitioning of Q_v between small and large pores is different at different pressures, equation (11) indicates that σ_{sf} will not be a constant. Thus, the assumptions implicit in applying equation (14) to experimental data may cause errors in the interpretation of PS_s and σ_{sf}.

Blake and Staub (4) analyzed lymph and protein flow data from the lungs by assuming a specific multiple pore structure (relative numbers of pores of specified size) for lung exchanging vessels. They found that a small pore ($\sigma_{si} = 1$), an intermediate sieving pore ($0 < \sigma_{si} < 1$) and a large pore ($\sigma_{si} = 0$) could describe lymph to plasma (L/P) ratios of albumin and grouped globulin fractions from experiments in unanesthetized sheep. Thus, the addition of a large pore to the system used by Renkin et al. (8, 9) obviated the necessity to include vesicular transport in order to describe lung L/P. Blake and Staub were less successful in the theoretical prediction of lymph flow rates.

Harris et al. (7, 25) used the multiple-pore approach to describe experimentally observed ratios of protein PS to urea PS derived from indicator dilution studies. They found a three-pore structure similar to the Blake and Staub (4) model adequate to describe these observations for eight protein fractions analyzed in lymph and plasma. However, they were unable to predict the observed L/P ratios with this structure.

A Computational Technique for Transport Coefficients Based on Multiple Pathways

Our model for lymph and protein transport in the lung is a variation of that proposed by Blake and Staub (4). The fundamental assumptions are:

- A significant fraction of protein, fluid and tracer molecules move through the same pore structure.
- Some tracer may diffuse through barriers which have insignificant convection.
- Some protein may be transported by vesicles.
- The capillary membrane undergoes passive transport due to hydrostatic concentration gradients; contains cylindrical pores; has a uniform thickness; has a constant relative number of pores of specified sizes per unit area of membrane.
- The interstitium has concentrations of solutes which are identical to their concentrations in the lymph draining the interstitium and is drained only by non-sieving lymph ducts.
- The intracapillary space has plasma protein concentrations identical to those measured in peripheral plasma; has a linear hydrostatic pressure drop from arteriole to venule which is uniform throughout the lungs.
- Restricted diffusion in pores is describable by hydrodynamic analogies.
- Convection and diffusion are thermodynamically coupled, but no diffusional cross-coupling between solutes occurs.

At steady-state it is assumed that lymph flow and lymph protein flow from the lung are equal to the lymph and lymph protein flows which cross the microvascular membrane. In particular, the fluid and solute flow equations through a single pore of radius R_{pi} for a number of solutes, s, is taken to be:

$$J_{vi} = L_i(\Delta P - \Sigma_s \sigma_{si} \Delta \pi_s) \tag{15}$$

$$J_{si} = PS_{si}(C_{sp} - C_{sL}) + (1 - \sigma_{si})\overline{C}_s J_{vi} \tag{16}$$

where $\overline{C}_s$ is defined by equations (3), (4) and (5).

The filtration coefficient for a single pore should be identical to the resistance for laminar flow in a circular tube,

$$L_i = \frac{\pi R_{pi}^4}{\Delta Z 8 \mu} \qquad (17)$$

where μ = viscosity of water and ΔZ = membrane thickness.

The permeability of a given solute s in a pore i is defined as

$$PS_{si} = F_s(\alpha) \kappa_1(\alpha) \frac{\pi R_{pi}^2 D_s}{\Delta Z} \qquad (18)$$

where $\alpha = a_s/R_{pi}$;
a_s = molecular radius of substance s;
D_s = binary diffusivity of protein s in water;

$F_s(\alpha) = (1-\alpha)^2$ the steric hinderance term;
$\kappa_1(\alpha)$ = Tabulated function from the numerical solution of the hydrodynamic problem (22).

The reflection coefficient is defined as:

$$\sigma_{si} = 1 - (F_{sf}(\alpha) \frac{\kappa_2(\alpha)}{\kappa_1(\alpha)} \qquad (19)$$

where $F_{sf}(\alpha) = 2(1-\alpha)^2 - (1-\alpha)^4$, the steric hinderance term for laminar flow;

κ_1, κ_2 = Tabulated functions resulting from solution of the hydrodynamic problem (published in reference 22).

If the vascular membrane is considered to consist of repeating groups of transport pathways which are uniform, then the fluid flow through such a "membrane transport unit" (MTU) is

$$Q_T = \Sigma_i n_i J_{vi}$$

and solute flow is

$$Q_s = \Sigma_i n_i J_{si} + J_{sD}$$

where n_i is the number of pores of size R_{pi} in an MTU and J_{sD} is the flux of solute s through pathways other than pores. The quantity J_{sD} could be a nonconvective pathway or vesicular movement for large proteins.

These expressions may be incorporated into a description of vascular transport for the entire lung. Under steady-state conditions,

$$Q_v = N_T Q_T \qquad (20)\cdot$$

and

$$C_{SL} Q_v = N_T Q_S \qquad (21)$$

where N_T is the number of membrane transport units in the lung and Q_v is the total lung lymph flow.

Experimental studies of pulmonary lymph in unanesthetized sheep provide two kinds of data which should be describable by an appropriate transport model: the L/P ratios for all fractions analyzed in the lymph and the fraction (η) of total lung lymph which was collected during the experiment.

The theoretical equation for L/P ratio is

$$\frac{C_{SL}}{C_{SP}} = \frac{(\Sigma_i n_i PS_{si}) + \Sigma_i n_i (1-\sigma_{si})(1-\Theta_{si})J_{vi} + K}{(\Sigma_i n_i PS_{si}) + \Sigma_i n_i [1-\Theta_{si}(1-\sigma_{si})] J_{vi} + K} \qquad (22)$$

where it is assumed that any non-convective large protein flow through a membrane transport unit (such as vesicular transport) is described by

$$J_{sD} = K(C_{sP} - C_{sL}) \qquad (23)$$

The collected fraction is defined as

$$\eta = \frac{\text{Observed lung lymph flow}}{\text{Total lung lymph flow}}$$

$$\eta = \frac{Q_o}{N_T \Sigma_i n_i J_{vi}}$$

The permeability surface area (PS_T) from multiple indicator data (if available) may be used to help calculate η if we assume that tracer injected in a multiple-indicator study passes through the same pores in a single pass as water and protein does in the steady-state. Thus:

$$N_T = \frac{PS_T}{\Sigma_i n_i PS_{Ti}}$$

and

$$\eta = \frac{Q_o \Sigma_i n_i PS_{Ti}}{PS_T \Sigma_i n_i J_{vi}} \qquad (24)$$

Anatomic data (12) shows that this fraction should be between .66 and 1.0 for the unanesthetized sheep preparation. This fraction

should remain the same for all experiments on a given sheep. If this is true then the model-predicted ratio of lymph flow after an experimental manipulation to lymph flow at baseline will agree with experimental observations. This can be seen after rearranging equation (24):

$$[Q_o = \eta \; \frac{PS_T}{\Sigma_i n_i PS_{Ti}} \quad \Sigma_i n_i J_{vi}] \quad \text{Baseline}$$

and

$$[Q_o = \eta \; \frac{PS_T}{\Sigma_i n_i PS_{Ti}} \quad \Sigma_i n_i J_{vi}] \quad \text{Manipulation}$$

If η is the same in both situations, dividing these two equations leads to

$$\frac{[Q_o]B}{[Q_o]M} = \frac{[PS_T \; \Sigma \; n_i J_{vi}/\Sigma_i \; n_i PS_{Ti}]B}{[PS_T \; \Sigma \; n_i J_{vi}/\Sigma_i \; n_i PS_{Ti}]M}$$

It is generally thought that membrane structure is not altered in the lung by moderate increases in left atrial pressure (1). Thus a set of data consisting of L/P values at baseline and after elevated pressure can provide a basis for selecting structural parameters. If eight protein fractions are available at two pressure levels then a total of 16 observations will provide a data base for structural identification. For three pore sizes and vesicular transport characterized by a single constant, a total of 6 parameters can be determined (3 pore radii, R_{pi}, two relative pore numbers n_i and a vesicular constant $\check{K}$). The following algorithm may be used:

1. Assume a pathway structure (n_i's, R_{pi}'s, K).

2. Compute theoretical L/P ratios from equation (22) for the available proteins.

3. Compute

$$\phi = \Sigma_s \frac{[(C_{SL}/C_{SP}) \text{ observed} - (C_{SL}/C_{SP}) \text{ predicted}]^2}{[C_{SL}/C_{SP}] \text{ observed}}$$

4. Repeat unitl ϕ is a minimum.

5. Compute η from equation (24).

6. Consider any structure with an acceptably low ϕ and $.66 < \eta < 1.0$ appropriate for the description of the experimental results.

Experimental Results

Figures 1 and 2 compare the steady-state responses of pulmonary vascular pressures, lung lymph flow and lymph/plasma protein concentration to histamine (5) and Pseudomonas (14) infusion with the responses to mechanically increased pressure (13). The histamine and Pseudomonas responses contrast to pressure effects in that lymph flow increases while lymph/plasma protein concentration remains high. The response to infusing E. coli endotoxin is very similar to the response to infusing whole Pseudomonas bacteria (14, 26). There is an initial phase where pulmonary artery pressure and lung lymph flow increase but lymph protein concentration falls, and a late steady-state phase with stable pulmonary vascular pressures and a high flow of protein rich lymph. These data are summarized and compared to increased pressure studies in Figure 3. As with histamine and Pseudomonas,
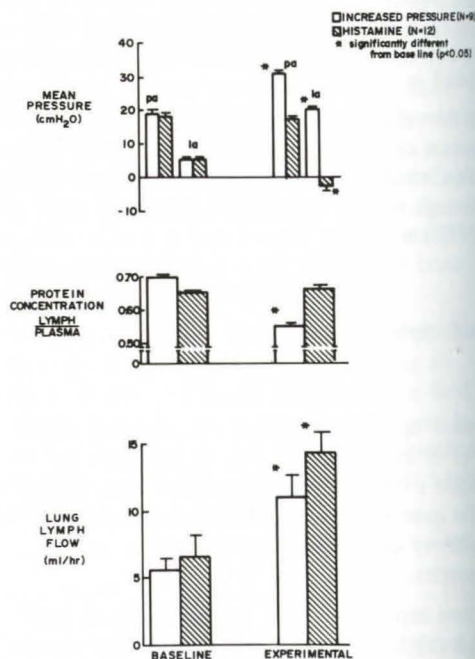

Fig. 1   Steady-state pulmonary vascular pressure and lung lymph responses to mechanically increased pressure (13) and intravenous histamine infusion (5) in unanesthetized sheep
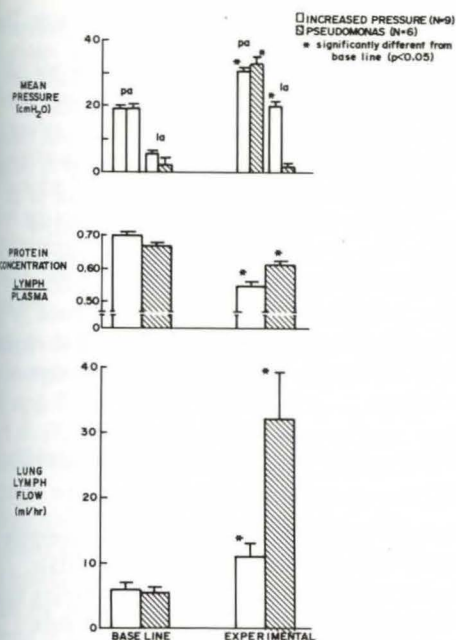
Fig. 2 Steady-state pulmonary vascular pressure and lung lymph responses to mechanically increased pressure (13) and intravenous *Pseudomonas aeruginosa* bacteria infusion (14) in unanesthetized sheep
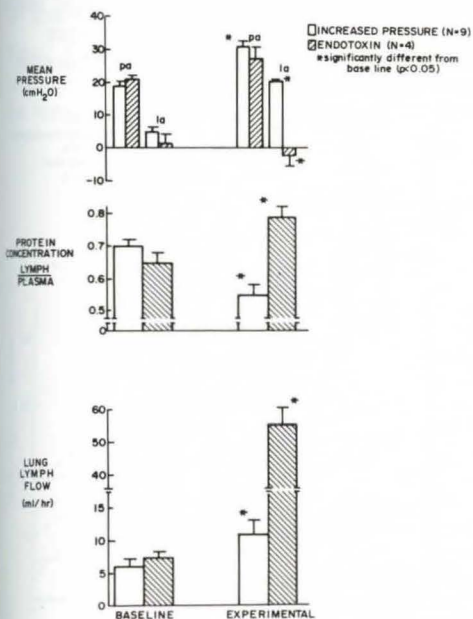

Fig. 3 Steady-state pulmonary vascular pressure and lung lymph responses to mechanically increased pressure (13) and intravenous *E. coli* endotoxin infusion in unanesthetized sheep

E. coli endotoxin has a different effect than elevating pressure: it causes high flow of protein rich lymph.

Lung lymph clearances (lymph flow x lymph/plasma concentration) of eight protein fractions is summarized for all of the studies in Figure 4. Clearance normally declines with increasing protein size and this relationship is preserved after pressure elevation even though clearance of all fractions increases slightly. Both histamine and Pseudomonas cause large increases in clearance of all fractions, but there is still decreasing clearance with increasing molecular size. Endotoxin increases clearance and reduces sieving of large protein molecules, indicated by less decline in lymph clearance as protein size increases.

To further illustrate the different patterns of the relationship between lung lymph protein clearance and molecular size, Figure 5 shows steady-state clearance for each experimental intervention normalized to baseline clearance as a function of protein molecular size. Increased pressure, histamine and Pseudomonas all cause relatively similar changes in clearance of each of the protein fractions. However, E. coli endotoxin causes a much greater relative increase in clearance of the larger fractions.
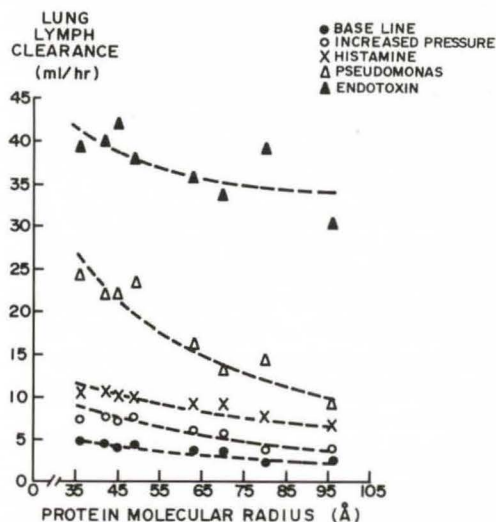

Fig. 4 Steady-state lung lymph clearance (lymph flow x lymph/plasma concentration) of eight protein fractions as a function of molecular size under several experimental conditions
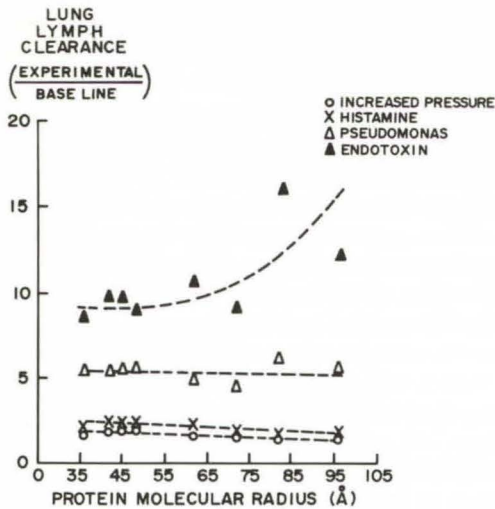
Fig. 5 Steady-state lung lymph clearance normalized to baseline for each of eight protein fractions as a function of molecular size for several experimental conditions

Discussion

Qualitative Conclusions About Permeability

We have contended that a qualitative conclusion about whether or not an experimental intervention changes lung vascular permeability can be made from steady-state lymph data by comparison with responses to mechanically increased pressure (5, 6). When pressure is increased, lung lymph flow increases and lymph/plasma protein concentration falls (5, 6, 27). That response is highly reproducible (5, 6, 27). But histamine, Pseudomonas and E. coli endotoxin all cause a steady state increase in lymph flow with no decrease in lymph/plasma protein concentrations. The increased fluid filtration cannot be accounted for by increased pressure and thus the resistance of exchanging vessel walls to fluid and protein movement must have decreased: permeability (in the general sense) must have increased.

The relationship between lung lymph clearance of proteins and their molecular radii also permits some qualitative conclusions about changes in lung microvessels. With histamine and Pseudomonas, lymph clearance is increased for all proteins, but clearance still

decreases as a function of molecular size. Thus, the structural changes in the walls of microvessels cannot be so large as to preclude sieving of proteins with radii less than 100 Å. E. coli endotoxin reduces, but does not eliminate sieving of proteins less than 100 Å radius. Endotoxin causes the lymph clearance of all proteins to increase and increases relative lymph clearance of larger proteins much more than that of smaller ones. The inference is that changes in lung microvessels caused by E. coli endotoxin are more severe than changes caused either by histamine or Pseudomonas infusion.

Quantitative Conclusions about Permeability PS$_s^\bullet$ For Various Conditions:

We have used several techniques to compute transport coefficients from the lung data. Figure 6 presents the results of applying equation (12) to all of the eight protein data shown in Figures 4 and 5. There is a general increase in PS$_s^\bullet$ with histamine, Pseudomonas and endotoxin infusions consistent with the inferences drawn from the clearance graphs. This calculation separates the histamine results from the increased pressure results more sharply than does computation of clearance.
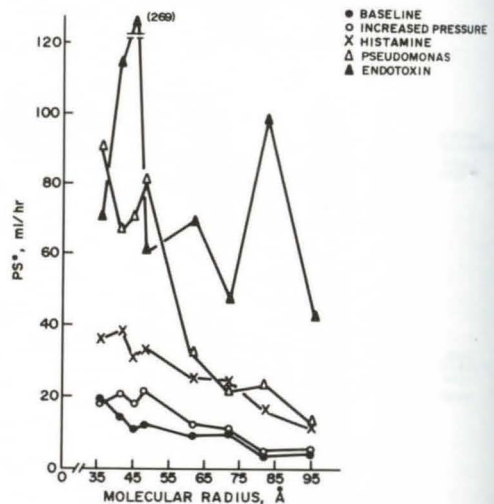

Fig. 6 Protein permeability-surface area computed from equation (12) for eight endogenous protein fractions under various experimental conditions

Increased Pressure Studies:

The *Renkin* et al. (8, 9) technique requires observations on the effects of increased micro-vascular pressure on a vascular bed with stable membrane properties. The $PS_s^\bullet$ results suggest that the baseline and increased pressure studies are such a system. Therefore, we have determined PS_s values from these data with both the *Renkin* method and a multiple pore model.

Figure 7 is a plot of $Q_V C_{SL}/(C_{SP} - C_{SL})$ for the eight protein fractions as a function of lymph flow. The hind limb data of *Renkin* et al. (8, 9) is included for comparison. The slopes (dependent upon σ_{pf}) generally decrease with increasing molecular radius as suggested by the theory. The intercepts (functions of both PS_p and σ_{pf}) vary considerably. The values of PS_s inferred from this method are shown in Figure 10. The trend is generally what would be expected for increasing molecular size but the PS_s values show considerable scatter. The PS_s values are smaller than those computed by equation (15) which are also shown (averaged for baseline and increased pressure).

Figure 8 shows a comparison of the *Renkin* hind limb σ_{pf} values to those computed from the lung data by the same technique. *Renkin*
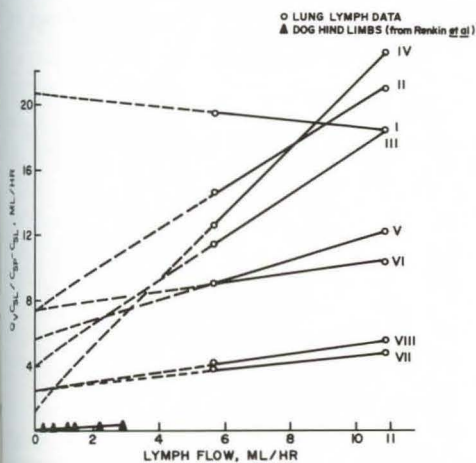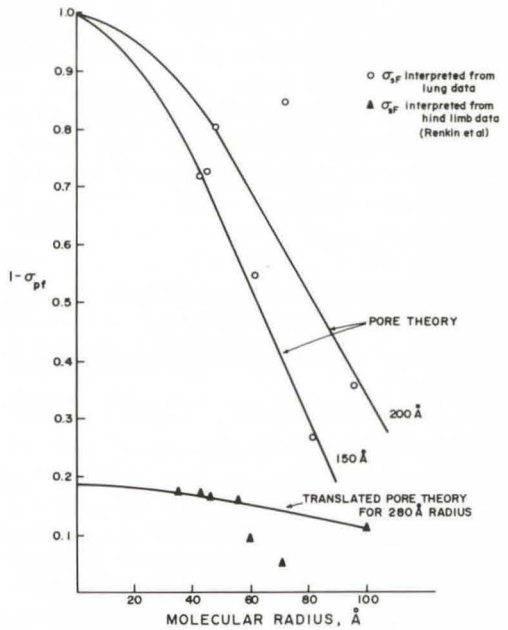

Fig. 8 Reflection coefficient computed from the slopes of the lines in Figure 7 as a function of molecular size. The results of applying the same method to hind limb data (reference 8) are included for comparison

et al. (8, 9) used the intercept of this plot to infer what fraction of lymph was carried through the large pore system. They found their data to intersect the ordinate at 0.185. This corresponded to a pore radius of 280 Å if the theoretical curves are translated to intersect at 0.185. For the lung data, the results are quite scattered but they suggest an intercept between 0.7 and 1 and a pore size between 200 Å and 150 Å.

We have used the multiple pathway model (neglecting vesicular transport) to determine a single optimal structure for the grouped baseline and increased pressure data. The predicted and observed L/P ratios are presented in Figure 9. Table 1 is a compilation of parameters resulting indicate that a membrane transport unit consiting of 3-pore sizes describes the data well. Pores of 40 Å, 140 Å and 1000 Å, with relative numbers 1.702×10^7, 1.225×10^4, and 1 respectively, make up the membrane transport unit. The model based lung PS_s values defined as

Fig. 7 Application of the *Renkin* et al. (8) equation (14) to lung and hind limb lymph data

$$PS_S = N_T\Sigma_i n_i PS_{si} \qquad (25)$$

are presented in Figure 10 for comparison with $PS_s^\bullet$ and *Renkin* PS_s values. These values are considerably smaller than those computed by the $PS_s^\bullet$ method. They roughly correspond to the *Renkin* PS_s values except for fraction I (albumin).

Their smaller size is plausible since the computation of $PS_s^\bullet$ includes convection and diffusion. The model results indicate that the fraction of purely diffusional flux ranges from about .15 (for fraction I) to .01 for the higher fractions.

Reflection Coefficients, σ_{sf}

Renkin et al. (8, 9) interpreted the σ_{sf} values computed from the slope of the $PS_s^\bullet$ vs. Q_L line to be that of a sieving "large pore". This restricted their pore system to intercellular and small intracellular pores ($\sigma = 1$) and a larger sieving pore. In our 3-pore model, we have considered small pores ($\sigma = 1$), sieving pores ($0 < \sigma < 1$) and large pores ($\sigma = 0$).

Figure 11 compares σ_{sf} for the lung computed by the *Renkin* technique with σ_{si} for the
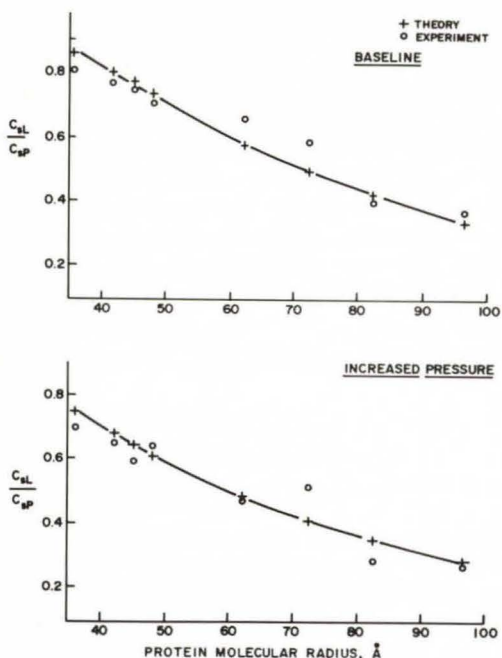
Fig. 9 Experimental and theoretical model values for lymph-to-plasma ratios of protein concentration from unanesthetized sheep lung studies as a function of molecular size

Tab. 1 Parameter Values Resulting From Analysis of Baseline and Increased Pressure Studies with the 3-Pore Theoretical Model

	Baseline Studies	Increased Pressure Studies
$R_p:n_i$	40 A: 1.702 x 10^7	(Same)
	140 A: 1.225 x 10^4	(Same)
	1000 A: 1	(Same)
J_{vi}/Q_v		
40 Å	0.080	0.193
140 Å	0.679	0.598
1000 Å	0.252	0.209
σ_{sF} (calculated from Equation 11)		
I	0.231	0.333
II	0.278	0.377
III	0.303	0.398
IV	0.327	0.420
V	0.443	0.522
VI	0.521	0.590
VII	0.590	0.651
VIII	0.669	0.720
Tissue Press, mm Hg	0	6.5
N_T	7.92 x 10^5	7.31 x 10^5
η	0.968	0.925

Filtration Coefficients and σ_{pd}:

Table 2 presents the results of computing L_o and σ_{pd} by various means. If σ_{pd} is assumed to be 1, the L values are negative (and implausible) for all of our experiments except increased pressure. If equation (6) is solved for L_o and σ_{pd} under the baseline and increased pressure situations, an L_o value of 0.91 and a σ_{pd} of 0.117 results. The multiple pore model results in substantially higher values. The σ_{pd} of .92 is comparable to that seen in other systems (13).

Critique of Quantitative Methods

The simple calculation of $PS_s^\bullet$ assumes $\sigma_{pf} = 1$ and neglects convective contributions to protein flux. Nevertheless, Figure 7 illustrates that it is of some utility in separating true microvascular permeability change from the effects of increased pressure. In comparison to other methods, it appears to greatly exaggerate the amount of diffusive transport.

Renkin et al. (8, 9) have attempted to correct for convection by using several venous pressures and computing PS_s and σ_{sf} from a presumably linear relation between $PS_s^\bullet$ and Q_L. The method does not appear to be applicable to our lung data for several possible reasons:

1. The slope and intercepts of the $PS_s^\bullet$ vs Q_L plot are dependent on only two points, not six as in the hind limb studies. This certainly
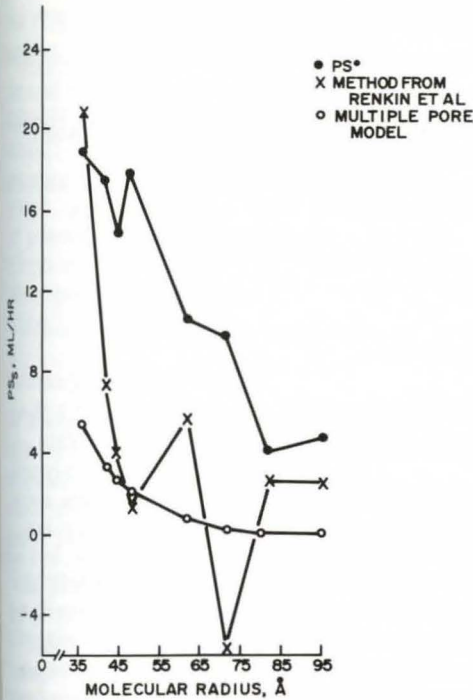
Fig. 10 Protein permeability surface-area computed by various methods as a function of molecular radius

intermediate pore in our 3-pore model. The slope technique shows considerable scatter but the values are generally comparable to the model values.
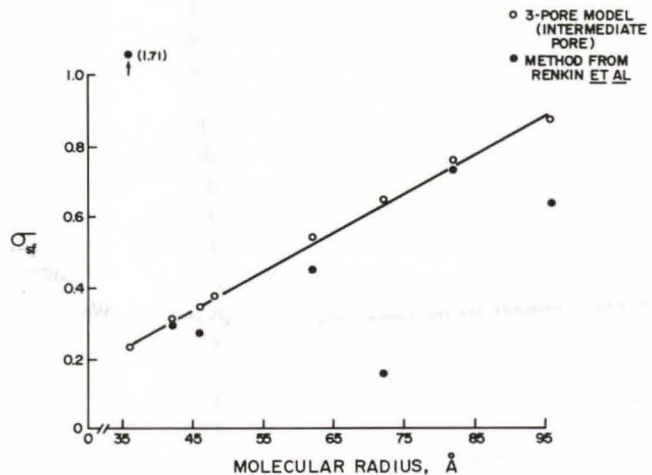
Fig. 11 Comparison of lung σ_{sf} determined by the Renkin method (8) to that determined for the intermediate pore by multiple-pore model analysis

Tab. 2 Total Filtration Coefficient (L_0) and Mean Reflection Coefficient (σ_{PD}) Computed by Various Techniques

	Method				
	Equation (16)	Equation (6)		Multiple Pore Model	
Experiment	$L^{\cdot}$ (g/hr x mm Hg)	L_0	σ_{PD}	L_0	σ_{PD}
Baseline	-2.54	0.91*	0.117*	10.76	0.923
Increased Pressure	3.72			9.80	0.919
Histamine	-3.40	–	–	–	–
Pseudomonas	-48.92	–	–	–	–
Endotoxin	-111.43	–	–	–	–

* Values computed from both baseline and increased pressure data.

contributes to the possibility of error in applying the method. However, it is technically difficult to vary microvascular pressure in a graded manner and achieve multiple steady states in the unanesthetized sheep preparation. High pressures can precipitate alveolar flooding, particularly in increased permeability situations. On the other hand, the lymph flow from the sheep experiments is considerably greater than that in the hind limb and possibly less susceptible to experimental error.

2. The fundamental assumptions of the *Renkin* et al. (12, 13) method are violated in the sheep experiments. As shown by equation (11), the value of σ_{pf} (and the slope of the lines in Figure 7) is only constant under different pressures and flows if the fraction J_{vi}/Q_v is constant for a given pore size. If relative flow shifts during an increased pressure experiment, then σ_{pf} must vary between a baseline and increased pressure experiment and the $PS_s^{\bullet}$ vs. Q_L relationship is not linear. The model results shown in Table 1 indicate that the relative fraction of flow changes from .08 through the small pores at baseline to 0.193 under increased pressure conditions. The resulting changes in σ_{pf} are also indicated. This may be the most important source of error in applying this technique to our data.

Values of filtration coefficient shown in Table 2 appear to be valid only if computed from the model. The average weight of drained wet lungs for our sheep was 385 g (28). This yields a value for L_0 of 2.06 ml/(hr x cmH$_2$O x 100 g tissue) which is comparable to that measured in isolated dog lobes (1).

The 3-pore model is a special case of a flow only ($\sigma = 1$) pathway, a restricted solute ($0 < \sigma < 1$) pathway and a plasma-to-lymph fluid shunt ($\sigma = 0$). The L/P ratios are quite sensitive to the sieving pore size. They are also sensitive to total large pore flow, but not the specific 1000 Å size. Any large leak size with a $\sigma = 0$ could be specified as long as its total flow, when combined with the other pore transport streams, produced the experimental L/P spectrum. This is less true of the small pore size. As in the case of large pores, any $\sigma = 1$ pore might be specified to produce the L/P ratios (as long as enough pores were defined to give the proper water flow). However, tracer PS_T predicted by the pore model is very sensitive to the small pore size. Thus, the collected fraction, η, is likewise sensitive to small pore radius and the 40 Å value was necessary to achieve the 0.93 to 0.96 fraction found by model analysis.

A notable characteristic of the model analysis was that no 3-pore structure could predict the L/P ratios for $\eta > .6$ with an interstitial pressure of 0 during increased vascular pressure. We were unable to fit the data with any 3-pore structure or by adding vesicular transport. A positive tissue pressure (6.5 mm Hg) was required to describe the data produced by increasing left atrial pressure.

We found that L/P ratio was not highly sensitive to vesicular transport as defined by equation (23). Further work is needed to assess the importance of this pathway. If vesicular transport is considered to be a pathway for both fluid and solute (instead of pure solute),

the large pore might be considered to be a pathway equivalent to vesicular action.

Several features of the theoretical analysis strongly support the utility of the 3-pore model: 1) it predicts baseline and increased pressure L/P ratios; 2) it predicts relative lymph flow at two conditions of microvascular pressure; 3) it agrees with the collected lymph fraction indicated by ^{14}C-urea permeability surface area measured by indicator dilution.

Summary and Conclusions

By measuring blood to lung lymph transport of several endogenous proteins under a variety of steady state conditions, it is possible to make qualitative and quantitative conclusions about the function of lung exchanging vessels.

When microvascular permeability is increased, the relationships between pulmonary vascular pressures, lymph flow and lymph/plasma protein concentrations are clearly different than when pulmonary vascular pressures are mechanically elevated, but microvascular permeability is unchanged. Lymph clearance of proteins with molecular radii 35.5 to 96 Å also increases more with increased permeability than with increased pressure but at least with histamine, Pseudomonas and E. coli endotoxin infusion in sheep, protein molecular sieving persists during increased permeability reflected in decreasing clearance with increasing protein size. Endotoxin causes a relatively greater increase in clearance of larger proteins than either histamine or Pseudomonas, suggesting more severe alterations in exchanging vessels.

There are difficulties in making quantitative inferences about microvascular function directly from lymph data. The simple calculation of solute permeability surface area products assuming totally diffusive flux (PS$^\bullet$) may have some utility, but the values are erroneously high, especially for smaller proteins, because of substantial transvascular convective flux. The more recently proposed method of Renkin et al. (8, 9) where microvascular reflection coefficients and permeability surface area products are inferred from

relationships between PS$^\bullet$ and lymph flow gives variable results from our lung data, possibly because the method assumes that overall membrane coefficients do not change with changing filtration rates. That assumption is untrue in a heteroporous membrane when changes in the partitioning of filtration among the various pores occurs.

An equivalent multiple pore mode, where the equations describing fluid and solute flux through porous media are used to predict experimental results, promises more specific information about exchanging vessels in the lung. The model analysis is supported by the fact that membrane coefficients calculated from it are similar to values measured more directly in the lung by other investigators. This approach may be the only way to make quantitative inferences about exchanging vessel transport in organs where transport of fluid and solutes occurs through multiple pathways which impose different restrictions on fluid and solute movement. This appears to be the case for the lung.

References

1 *Staub, N.:* Pulmonary edema. Physiol. Rev. 54 (1974) 678
2 *Vriem, C., P. Snashall, R. Demling, N. Staub:* Lung lymph and free interstitial fluid protein composition in sheep with edema. Am. J. Physiol. 230 (1976) 1650
3 *Nicolaysen, G., A. Nicolaysen, N. Staub:* A quantitative radioautographic comparison of albumin concentration in different sized lymph vessels in normal lungs. Microvasc. Res. 10 (1975) 138
4 *Blake, L., N. Staub:* Pulmonary vascular transport in sheep: A mathematical model. Microvasc. Res. 12 (1976) 197
5 *Brigham, K., P. Owen:* Increased sheep lung vascular permeability caused by histamine. Circ. Res. 37 (1975) 647
6 *Brigham, K., P. Owen:* Mechanism of the serotonin effect on lung transvascular fluid and protein movement in awake sheep. Circ. Res. 36 (1975) 761
7 *Harris, T., C. Woltz, K. Brigham:* The inference of pulmonary capillary permeability from lymph and multiple indicator experiments: Comparison with equivalent pore theory. Proc. 29th Ann. Conf. Engr. Med. Biol. 18 (1976) 228
8 *Renkin, E., W. Joyner, C. Sloop, P. Watson:* Influence of venous pressure on plasma-lymph transport in the dog's paw: Convective and dissipative mechanisms. Microvasc. Res. 14 (1977) 191

9 Renkin, E., P. Watson, C. Sloop, W. Joyner, F. Curry: Transport pathways for fluid and large molecules in microvascular endothelium of the dog's paw. Microvasc. Res. 14 (1977) 205

10 Taylor, A., N. Granger, R. Braece: Analysis of lymphatic protein flux data. I. Estimation of the reflection coefficient and permeability surface area product for total protein. Microvasc. Res. 13 (1977) 297

11 Brace, R., N. Granger, A. Taylor: Analysis of lymphatic protein flux data. II. Effect of capillary heteroporosity on estimates of reflection coefficients and PS products. Microvasc. Res. 14 (1977) 215

12 Staub, N., R. Bland, K. Brigham, R. Demling, J. Erdmann, W. Woolverton: Preparation of chronic lung lymph fistulas in sheep. J. Surg. Res. 19 (1975) 315

13 Bowers, R., K. Brigham, P. Owen: Salicylate pulmonary edema: The mechanism in sheep and review of the clinical literature. Am. Rev. Resp. Dis. 115 (1977) 261

14 Brigham, K., P. Owen, R. Bowers: Increased permeability of sheep lung vessels to proteins after Pseudomonas bacteremia. Microvasc. Res. 11 (1976) 415

15 Failing, J., M. Buckley, C. Zak: Automatic determinations of serum proteins. Amer. J. Clin. Pathol. 33 (1960) 83

16 Renkin, E.M.: Brief Reviews: Multiple pathways of capillary permeability. Circ. Res. 41 (1977) 735

17 Kedem, O., A. Katchalsky: Thermodynamic analysis of the permeability of biological membrane to non-electrolytes. Biochem. Biophys. Acta. 27 (1958) 229

18 Solomon, A.K.: Characterization of biological membranes by equivalent pores. J. Gen. Physiol. 51 (1968) 335s.

19 Bean, C.P.: Physics of porous membranes. In: C. Esenman (ed.) Membranes: A series of advances. Vol. 7, pp. 1–54, New York: Dekker, 1972

20 Levitt, D.G.: Kinetics of diffusion and convention in 3.2 Å pores. Exact solution by computing simulation. Biophysical J. 13 (1973) 186

21 Anderson, J.L., J.A. Quin: Restricted transport in small pores. A model for steric exclusion and hindered particle motion. Biophysical J. (1974) 130

22 Paine, P.L., P. Scherr: Drag coefficients for movements at rigid spheres through liquid filled cylindrical pores. Biophys. J. 15 (1975) 1087

23 Lightfoot, E.N., J.B. Bassingthwaighte, E.F. Grabowski: Hydrodynamic models for diffusion in microporous membranes. Ann. Biom. Engr. 4 (1976) 78

24 Patlak, C.S., D.A. Goldstein, J.F. Hoffman: The flow of solute and solvent across a two membrane system. J. Theor. Biol. 5 (1963) 426

25 Harris, T.R.: Lung microvascular permeability: Transport theory and measurement methods, Advances in Biomedical Engineering, C. Cooney, ed., Dekker, in press

26 Brigham, K., W. Woolverton, L. Blake, N. Staub: Increased sheep lung vascular permeability caused by Pseudomonas bacteremia. J. Clin. Invest. 54 (1974) 792

27 Erdmann, J., T. Vaughan, K. Brigham, W. Woolverton, N. Staub: Effect of increased vascular pressure on lung fluid balance in unanesthetized sheep. Circ. Res. 37 (1975) 271

28 Harris, T.R., K.L. Brigham, R.D. Rowlett: Pressure, serotonin and histamine effects on lung multiple-indicator curves in sheep. J. Appl. Physiol. 44 (1978) 245

Dr. Kenneth L. Brigham, Room B-3211, Vanderbilt University Hospital, Nashville, Tennessee 37232